Science of the Total Environment xxx (2017) xxx–xxx

Contents lists available at ScienceDirect

Science of the Total Environment

journal homepage: www.elsevier.com/locate/scitotenv

Rhamnolipid-aided biodegradation of carbendazim by *Rhodococcus* sp. D-1: Characteristics, products, and phytotoxicity

Naling Bai [a], Sheng Wang [a], Rexiding Abuduaini [a], Meinan Zhang [a], Xufen Zhu [b], Yuhua Zhao [a,*]

[a] Institute of Microbiology, College of Life Sciences, Zhejiang University, Hangzhou 310058, PR China
[b] Institute of Genetics, College of Life Sciences, Zhejiang University, Hangzhou 310058, PR China

HIGHLIGHTS

- *Rhodococcus* sp. D-1 was isolated as an efficient MBC-degrading bacterium.
- Genome of D-1 was analyzed and the general MBC biodegradation pathway was proposed.
- Rhamnolipid promoted MBC biodegradation and detoxification in a concentration-dependent manner.
- Emulsification and favorable changes in cell surface characteristics facilitated MBC degradation of D-1.

GRAPHICAL ABSTRACT

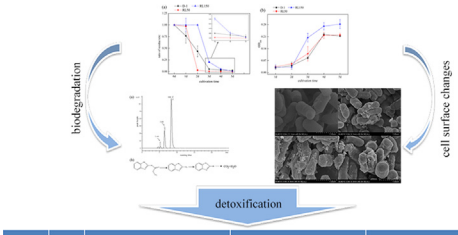

	CK_{MM}	0 d			2 d			3 d		
		RL0	RL50	RL150	RL0	RL50	RL150	RL0	RL50	RL150
Germination percentage	93±7	97±5	90±1	69±1**	84±1	97±1	73±19*	83±4	81±0	79±12
Shoot length (cm)	1.23±0.13	0.4±0.14***	0.175±0.11***	0.25±0.07***	0.3±0.18***	0.55±0.07**	0.15±0.07***	0.8±0.28*	1.125±0.18	0.85±0.49
Root length (cm)	0.5±0.13	0.125±0.11**	0.05±0.07***	0.1±0.14**	0.2±0.28*	0.45±0.07	0.125±0.04**	0.45±0.07	0.7±0.01	0.275±0.18*

ARTICLE INFO

Article history:
Received 1 January 2017
Received in revised form 2 March 2017
Accepted 3 March 2017
Available online xxxx

Editor: Jay Gan

Keywords:
Carbendazim
Rhamnolipid
Biodegradation
Cell surface hydrophobicity
Zeta potential
Detoxification

ABSTRACT

We successfully isolated *Rhodococcus* sp. D-1, an efficient carbendazim-degrading bacterium that degraded 98.20% carbendazim (200 ppm) within 5 days. Carbendazim was first processed into 2-aminobenzimidazole, converted to 2-hydroxybenzimidazole, and then further mineralized by subsequent processing. After genomic analysis, we hypothesized that D-1 may express a new kind of enzyme capable of hydrolyzing carbendazim. In addition, the effect of the biodegradable biosurfactant rhamnolipid on the rate and extent of carbendazim degradation was assessed in batch analyses. Notably, rhamnolipid affected carbendazim biodegradation in a concentration-dependent manner with maximum biodegradation efficiency at 50 ppm (at the critical micelle concentration, CMC) (97.33% degradation within 2 days), whereas 150 ppm (3 CMC) rhamnolipid inhibited initial degradation (0.01%, 99.26% degradation within 2 and 5 days, respectively). Both carbendazim emulsification and favorable changes in cell surface characteristics likely facilitated its direct uptake and subsequent biodegradation. Moreover, rhamnolipid facilitated carbendazim detoxification. Collectively, these results offer preliminary guidelines for the biological removal of carbendazim from the environment.

1. Introduction

Carbendazim (Methyl-1*H*-Benzimidazol-2-ylcarbamate, MBC) is a stable benzimidazole fungicide widely used to control fungal disease; however, stability and soil persistence can lead to long-term contamination, as its chemical structure favors adsorption into the soil matrix and

* Corresponding author.
E-mail address: yhzhao225@zju.edu.cn (Y. Zhao).

http://dx.doi.org/10.1016/j.scitotenv.2017.03.025
0048-9697/

accumulation following repeated applications (Lewandowska and Walorczyk, 2010). MBC is also reported to disrupt the human endocrine system and contribute to serious estrogen-mediated pathologies (Morinaga et al., 2004), as well as damage the mammalian liver, endocrine, and reproductive tissues even at low doses (Zhang et al., 2013). Moreover, the persistence of MBC in soil alters the biodiversity of bacterial communities and adversely affects microbial functions (Singh et al., 2016; Wang et al., 2009). The half-life of MBC ranges from several days to 12 months depending on the nature of the soil (Singh et al., 2016). Thus, recognition of MBC's toxigenic, mutagenic, and teratogenic effects has impelled research on its removal from the environment.

Bioremediation is a promising method to dispose refractory pollutants due to its eco-friendliness, high-efficiency, and domestication (Holtman and Kobayashi, 1997). Notably, MBC is not significantly degraded by sunlight radiation (Salunkhe et al., 2014). Recently, several microorganisms have been reported to degrade MBC, including *Nocardioides* sp. (Pandey et al., 2010), *Rhodococcus erythropolis* (Holtman and Kobayashi, 1997; Jing-Liang et al., 2006; Zhang et al., 2013), *Pseudomonas* sp. (Fang et al., 2010; Lei et al., 2016), *Bacillus subtilis* (Salunkhe et al., 2014), and some fungal stains. However, no reports exist on enzymes closely related to MBC biodegradation pathway, with the exception of MBC-hydrolyzing esterase MheI, which metabolized MBC to 2-aminobenzimidazole (2-AB) (Pandey et al., 2010).

Meanwhile, the effectiveness of biodegradation of this hydrophobic pollutant is limited by its actual bioavailability owing to the aqueous/non-aqueous biphasic nature of the system and interactions with large molecules in soil (Lewandowska and Walorczyk, 2010). Recent studies demonstrate that surfactants enhance bioavailability through various mechanisms such as emulsification, micellar solubilization, and facilitated mass transport (Mohanty and Mukherji, 2012). Emulsification may enhance the pollutant's solution rate and direct interfacial uptake. In contrast, micellar solubilization segregates hydrocarbons into a hydrophobic core when above the surfactant's critical micelle concentration (CMC), resulting in micelles with a hydrophilic surface and increased aqueous solubility (Mohanty and Mukherji, 2013). The effectiveness of hydrocarbon biodegradation can be optimized using chemical surfactants or biosurfactants in a manner dependent on the inherent characteristic of the surfactant and type of pollutant (Guha and Jaffé, 1996; Fernando Bautista et al., 2009; Chang et al., 2015). Tween 80, Triton X-100, and Tergitol NP-10 may improve the biodegradation process by increasing solubility and bioavailability above CMC (Fernando Bautista et al., 2009). Rhamnolipid (RL) solutions can potentially modify the cell surface hydrophobicity (CSH) to facilitate bacterial transport (Zhong et al., 2016a). Some chemical surfactants may result in secondary contamination due to increased biodegradation resistance and stability (Mohanty and Mukherji, 2012). Moreover, some biosurfactants may compete with pollutants as a source of carbon and energy or disturb the homeostasis of hydrocarbon-degrading microorganisms due to their antibacterial properties. The partially degraded surfactants would result in a significant reduction of surface-active and micellar solubilization capacities (Lee et al., 2013). β-Cyclodextrin tends to form stable inclusion complexes with contaminants that may either promote or inhibit the biodegradation process (Zhang et al., 2012). The value of hydrophile-lipophile balance obtained for RL was lower than that for sodium dodecyl sulfate, indicating higher emulsification and solubilization capacity for hydrophobic pollutants. Moreover, some RL homologs contain a larger micelle volume with two hydrophobic alkyl groups, and thus hold more pollutant molecules (Pornsunthorntawee et al., 2009). Notably, the polarity and solubility properties of contaminants would affect the partition and mobility even with a high dose of surfactant (Sánchez-Camazano et al., 1995). As for polar pollutants, the solubilization is complicated since they are soluble in both the micelle core and hydrophilic groups, and interact with the water molecules bound to hydrophilic chains by hydrogen bonding (Dai and Dong, 1999). Surfactants are also more effective in solubilizing pollutants with larger octanol/water partition coefficient values and relative water insolubility (Dai and Dong, 1999; Zhou and Zhu, 2007). Thus, extensive analyses should be performed to identify the optimal surfactant class and dose prior to application.

Earlier studies have mostly focused on the role of surfactants in the degradation of polycyclic aromatic hydrocarbons (PAHs) and alkanes. Here, we delineate the mechanism of action of RL for biodegradation of the powdered pesticide MBC by gram-positive *Rhodococcus* sp. D-1. Cellular characteristics were monitored to gain deeper insights into the process of surfactant-mediated MBC microbial biodegradation, which will likely have important implications on the field of surfactant-aided bioremediation.

2. Materials and methods

2.1. Chemicals and microorganisms

MBC (97% purity), 2-AB, benzimidazole (BM) were purchased from Sigma-Aldrich (St. Louis, MO, USA). 2-hydroxybenzimidazole (2-HB) was obtained from J&K Scientific Ltd. (Shanghai, China). RL (90% purity) was from Gemking Biotechnology Ltd. (Huzhou, China). Enzymes used in this study were from Takara (Dalian, China).

2.2. Isolation of the MBC-degrading bacterium D-1

Samples for microorganism enrichment were collected from MBC-contaminated farmland in Wenzhou, Zhejiang, China. MBC-degrading bacteria were isolated by continuous transfer cultivation for almost two months. The D-1 strain was isolated for its ability to utilize MBC as the sole carbon and energy source, and it could form a transparent zone on minimum salt medium (MSM) agar. The 16S rDNA sequence was aligned with those of other related organisms retrieved from the NCBI in Clustal X, and phylogenetic tree was constructed by neighbor-joining method using MEGA4.0 Software (Tamura et al., 2007). Meanwhile, the degradation capacity on other specific compounds was also investigated.

2.3. MBC biodegradation by Rhodococcus sp. D-1

For biodegradation and growth studies, D-1 was cultured in multiple batch flasks containing 20 mL MSM with 200 ppm MBC. Flasks with an initial optical density measured at $\lambda_{600\ nm}$ (OD_{600}) = 1.0 were incubated in a rotary shaker in the dark at 200 rpm and 30 °C. Flasks were withdrawn at each time interval for up to 5 days to determine the amount of MBC remaining in the liquid medium. Biomass was estimated based on OD_{600} readings from a 7230G spectrophotometer (Mapada, Shanghai, China). MBC residue was extracted twice with a 4:1 solution of chloroform and acetone with an extraction ratio of 1:1. The aqueous phase was acidified to pH 2.0 with HCl before the second extraction. The collected organic layers were evaporated, and the remaining residue was redissolved in 15 mL solution of 1:2 methanol and chloroform. Samples were stored at −20 °C until high performance liquid chromatography (HPLC) analysis.

The metabolites produced during MBC biodegradation were also analyzed. Cultures grown in MSM supplemented with MBC were harvested at 0, 6, 12, 24, 48, 72, 96, and 120 h. Moreover, to further elucidate the metabolic pathway, the D-1 strain was cultivated with 2-AB as the sole carbon source and energy source and analyzed after culturing in the dark for 0, 5, 8, 12, 24, and 48 h. The HPLC was equipped with an Eclipse C18 column (250 × 4.6 mm × 5 μm; Agilent Technologies, Santa Clara, CA, USA) and a UV–Vis detector. Quantitative analysis of MBC was performed with an isocratic elution solution comprised of 85:15 methanol and water with a 0.8 mL/min flow rate at 280 nm wavelength. Alternatively, metabolites were assessed using a 60:40 solution of methanol and water containing 0.1% acetate acid and 0.1% triethylamine as the mobile phase, at a flow rate of 0.5 mL/min and wavelength of 280 nm. BM, 2-HB, and 2-AB standards were also analyzed as references.

Please cite this article as: Bai, N., et al., Rhamnolipid-aided biodegradation of carbendazim by *Rhodococcus* sp. D-1: Characteristics, products, and phytotoxicity, Sci Total Environ (2017), http://dx.doi.org/10.1016/j.scitotenv.2017.03.025

2.4. Genome sequencing and MBC hydrolyzing enzyme analysis

Genomic DNA was isolated with the EasyPure Genomic DNA kit (TransGen, Beijing, China), subjected to quality control by agarose gel electrophoresis, and then quantified with a Micro-Spectrophotometer K5600. Library construction and sequencing was performed at the Novogene Bioinformatics Technology Co. Ltd. (Beijing, China). The *Rhodococcus* sp. D-1 genome was analyzed by whole-genome shotgun sequencing strategy with Illumina Hiseq 4000 paired-end sequencing and assembled using SOAP*denovo*. All reads were used for further gap closure, and gene prediction was performed with GeneMarkS (Besemer et al., 2001). Protein-coding genes were predicted using GeneMarkS, whereas tRNA, rRNA, and sRNA sites were examined by tRNAscan-SE (Lowe and Eddy, 1997), rRNAmmer (Lagesen et al., 2007), and Rfam (Gardner et al., 2009), respectively. A whole genome BLAST search was performed against 6 databases, namely, KEGG, COG, NR, Swiss-Prot, GO, and TrEMBL. We also searched for the reported MheI esterase sequences (ACV42481 and AEA07594) in the entire sequenced D-1 genome.

2.5. MBC biodegradation studies in presence of RL

D-1 was cultivated in 20 mL MSM containing 200 ppm MBC as the sole carbon source in the presence of increasing concentrations of RL (0, 50, and 150 ppm). First, 100 μL of 40 g/L MBC in acetone was spread onto the bottom of sterilized empty flasks and incubated in a horizontal shaker at 30 °C and 60 rpm for 2 h until the acetone was completely evaporated. After washed with sterile water, D-1 was added to the medium at an initial OD_{600} of 1.0. The D-1 growth and MBC degradation rates were analyzed with OD_{600} and HPLC, respectively. D-1 growth in the presence of RL in MSM without MBC was also examined as control.

2.6. MBC emulsification and solubilization by RL

Emulsification analysis was performed as previously described with some modifications (Mohanty and Mukherji, 2013). Briefly, increasing concentrations of MBC (100, 200, and 400 ppm) were added to batch flasks followed by MSM containing 50 or 150 ppm RL (CMC of RL is 50 ppm), respectively. Control experiments with only either RL or MBC were also performed. Samples were incubated in a shaker at 30 °C and 200 rpm for 2 days. A 1-mL culture sample was harvested and monitored for absorbance at 500 nm to analyze emulsification.

The effect of RL on MBC solubility was determined in the presence and absence of RL as previously described (Zhang et al., 1997). For each experiment, 200 ppm MBC was added into MSM as described above. After different doses of RL (0, 50, 150, 500, and 1000 ppm) were supplemented, samples were incubated in a 200 rpm shaker at 30 °C. Samples (1 mL) were withdrawn from each flask and filtered with a 0.45-μm membrane filter to remove any solid MBC particles, leaving a filtrate containing the aqueous MBC solubilized by different concentrations of RL. MBC concentrations were determined by HPLC analysis.

2.7. Analysis of cell surface characteristics

2.7.1. Determination of cell surface hydrophobicity

Bacterial CSH was measured by spectrophotometry (Zhang et al., 2012) and water contact angle analysis (Mohanty and Mukherji, 2012) to yield a relative measure of bacterial adherence to non-aqueous phase liquids. Cells were collected by centrifugation at 10,000 × *g* for 10 min, washed twice with sterilized water, and then re-suspended in the same solution to $OD_{400} = 0.6$. A 4.0-mL aliquot of bacterial suspension was mixed with 1.0 mL of n-hexadecane and vortexed for 60 s. The solution was allowed to rest for 30 min at room temperature, after which the sublayer was gently collected with 1-mL syringe and measured at OD_{400} with water as the blank control. We also monitored CSH by water contact angle analysis on bacterial mats prepared on filter membranes (0.45-μm cellulose acetate membranes). Harvested cell samples were washed and resuspended in sterilized water to $OD_{600} = 0.5$, and then 5 mL of the cell suspension was filtered to generate a bacterial mat. The filter was placed on LB agar plates for moisture standardization and drying. At least three contact angle measurements were conducted at various locations on each bacterial mat using a goniometer (KSV Co., Ltd., Helsinki, Finland).

2.7.2. Change of zeta potential

Zeta potential was measured using ZetaSizer Nano-ZS Zen 3600 (Malvern, England) to determine the change of cell surface charge as previously described with some modifications (Mohanty and Mukherji, 2012). Samples were prepared in sterile conditions. Briefly, cells were harvested by centrifugation at 10,000 × *g* for 15 min, washed three times with MSM, and the thalli were resuspended and adjusted the $OD_{400} = 0.5$ (Zhong, 2008). Samples were stored at 4 °C until analysis at a natural pH.

2.7.3. Scanning electron microscopy (SEM) analysis

SEM was performed on bacteria grown in MSM supplemented with 200 ppm MBC and 0, 50, and 150 ppm RL. Cells were harvested after 4 days of cultivation, washed three times with PBS buffer (pH 7.2), and fixed in 2.5% glutaraldehyde overnight at 4 °C. Afterwards, dried samples were then prepared and imaged using a JEOL JSM5600 LV scanning electron microscope (JEOL, Japan) (Sun et al., 2015). Cells cultivated in LB for 30 h were processed similarly and used as control group.

2.7.4. Fourier transform infrared spectroscopy (FTIR) analysis

FTIR analysis of cell surface functional groups was performed to further identify the mechanism of action of RL on MBC degradation. Cells cultivated for 5 days were harvested, washed twice with sterilized MSM, and pelleted at 10,000 × *g* for 15 min. Precipitates were freeze-dried for 20 h with a working temperature below −50 °C in a vacuum freeze drier (LABCONCO, Kansas City, MO, USA). Samples were scanned in the 4000–500 cm^{-1} region using an FTIR spectrophotometer (Nicolet AVtAR 370, Thermo Scientific, Waltham, MA, USA).

2.8. Phytotoxicity analysis

Phytotoxicity testing was performed to evaluate the toxicity of MBC and its degradation products on Chinese cabbage (*Brassica pekinensis*) seeds. D-1 was cultured in 20 mL MSM with 200 ppm MBC as the sole carbon source with RL (0, 50, and 150 ppm). Samples were harvested on Days 0, 2, and 3, and sterilized to avoid the influence of D-1. After centrifugation at 10,000 × *g* for 10 min, the suspensions were used as degradation solutions for phytotoxicity assays. Flasks without MBC served as controls. Pre-sterilization was performed as follows: the seeds were soaked in a 5% hydrogen peroxide solution for 5 min, and then washed with sterile distilled water 3 times for 3–5 min. Thirty seeds were then uniformly placed into a plate with 8 mL of degradation solution. All seeds were cultivated at 25 °C with 65% humidity under a light/dark cycle of 14 h/10 h. Shoot length, root length, and germination percentage were then analyzed after 5 days of cultivation.

3. Results and discussion

3.1. Identification of the MBC-degrading strain D-1

The D-1 bacterium was isolated in plate-clearing assay based on its ability to utilize MBC as the sole carbon source and energy source up to concentrations of 1000 ppm. The strain was gram-positive, rod-shaped, and formed orange-red colonies on LB agar after 2 days of cultivation at 30 °C. The 16S rDNA fragment sequence showed highest similarity with *Rhodococcus erythropolis* FS49 (Fig. 1). *Rhodococcus* species have an extraordinary capacity for metabolizing recalcitrant

Please cite this article as: Bai, N., et al., Rhamnolipid-aided biodegradation of carbendazim by *Rhodococcus* sp. D-1: Characteristics, products, and phytotoxicity, Sci Total Environ (2017), http://dx.doi.org/10.1016/j.scitotenv.2017.03.025

Fig. 1. Phylogenetic analysis of *Rhodococcus* sp. D-1 and other related species based on 16S rDNA sequences by Neighbor-joining method. Bootstrap values (percentages of 1000 replications) are shown at branch points. Scale bars represent 0.02 substitutions per nucleotide position. The accession numbers are in parentheses.

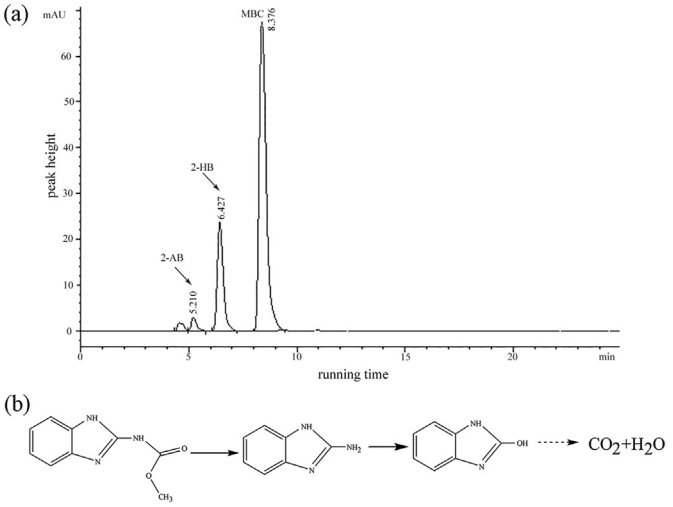

Fig. 2. (a) HPLC analysis of MBC and intermediates produced by D-1. (b) Proposed MBC metabolic pathway on the basis of intermediates detection. Dashed arrow: reactions supposed to be present during biodegradation period.

compounds, such as polycyclic aromatic compounds, halogenated aromatics, and amino- and nitro-derivatives of aromatic compounds and pesticides, as well as desulfurize coal and petroleum products (Jing-Liang et al., 2006; Martínková et al., 2009); thus, bioremediation with these strains will be practical and promising for cleaning-up of various pollutants (Table 1). Furthermore, *Rhodococcus* sp. D-1 decolored solutions of malachite green, methyl orange, crystal violet, and Congo red (data not shown). Strain D-1 may act as a promising candidate for MBC bioremediation in the environment.

3.2. Metabolic analysis in Rhodococcus sp. D-1

Two major metabolites, 2-AB and 2-HB, were detected out during MBC biodegradation (Fig. 2a). 2-AB is a highly toxic component that binds spindle microtubules, resulting in nuclear division arrest (Yenjerla et al., 2009). Interestingly, 2-AB was produced prior to 2-HB. Throughout the analysis period, only a slight amount of 2-AB was produced, whereas the relative content of 2-HB reached its maximum after 2 days of cultivation and diminished rapidly thereafter (Fig. S1). 2-HB formation was also detected during 2-AB biodegradation, indicative of progressive degradation. However, BM was not detected in either reaction, confirming a previous study with *Rhodococcus* sp. djl-11 (Zhang et al., 2013). Notably, differences in the conversion rate of 2-AB and 2-HB identified the former transformation reaction as the rate-limiting step; and 2-HB was then progressively degraded to CO_2 and H_2O by other enzymes in a stepwise way (Fig. 2b) (Fang et al., 2010).

3.3. Genome analysis and MBC-hydrolyzing enzyme prediction

Analysis of the D-1 genome revealed 57 contigs (>500 bp in size) with an N_{50} length of 540,370 bp. The draft genome sequence was 7.31 Mb, with a G + C content of 62.32%. There were 6690 predicted genes, 55 tRNAs, and 2 sRNAs. Of these, 697 genes were speculated to be involved in the degradation of xenobiotics, thus demonstrating its role in various xenobiotics degradation profiles and the necessity in exploration relative genetic resources in D-1. The draft genome sequence of *Rhodococcus* sp. D-1 has been deposited at GenBank under the accession number MNP00000000.

MheI (GQ454794) was identified to be involved in the first step of MBC transformation in *Nocardioides* sp. SG-4G by hydrolyzing MBC to 2-AB (Pandey et al., 2010). Notably, Zhang et al. (2013) analyzed the putative MBC-hydrolyzing esterase gene from *Rhodococcus erythropolis* dj1–11, which showed 99% sequence homology to the *MheI* (GQ454794). However, it was deficient in further corresponding verification. Since these three bacteria all metabolized MBC to 2-AB in the first step, we attempted to identify the MBC-metabolizing enzymes. Significantly, D-1 showed high similarity in 16S rDNA sequence identity with the djl-11 strain (Fig. 1), but we failed to amplify the *MheI* loci in *Rhodococcus* sp. D-1 using the referred primers MheI-F/MheI-R (Zhang et al., 2013). Thereafter, we queried the whole D-1 genome for the reported esterase MheI (ACV42481 and AEA07594), but only found a sequence with 35% identity in scaffold 4. After BLASTx, the deduced sequence showed 100% identity with alpha/beta hydrolase in *Rhodococcus*, which catalyzes the hydrolysis of substrates with different chemical composition or physicochemical properties using a nucleophile-His-acid catalytic triad. This hydrolysis often involves a nucleophilic attack on a carbonyl carbon atom; therefore, we hypothesized that the strain D-1 possessed a novel hydrolase activity distinct from MheI to hydrolyze MBC to 2-AB. Further work needs to be done to analyze enzymes involved in MBC biodegradation and detail the metabolic pathway.

Table 1
Substrate specificity of *Rhodococcus* sp. D-1 in MSM.

Substrate	Growth	Substrate	Growth	Substrate	Growth
Glucose	+	Toluene	+	Diphenyl ether	−
Dimethyl succinate	+	Nonylphenol Polytheoxylate (n_{ave} = 10)	+	4-Bromodiphenyl ether	−
4-Nonylphenol diethoxylate	+	3,4-Dimethybenzyl alcohol	+	Carbazole	−
Nonylphenol	+	Cholesterol	+	Biphenyl	−
Benzoic acid	+	*o*-Aminophenol	+	Dibenzofuran	−
Phenol	+	*p*-Bromophenol	−	Octane	−
Dodecane	+	Phenanthrene	−	Anthracene	−
Piperonyl butoxide	+	Naphthalene	−	Benzene	−

+: positive for *Rhodococcus* sp. D-1 growth in MSM with tested compounds as the sole carbon source; −: negative for growth in these conditions. MSM, minimal salt medium.

Please cite this article as: Bai, N., et al., Rhamnolipid-aided biodegradation of carbendazim by *Rhodococcus* sp. D-1: Characteristics, products, and phytotoxicity, Sci Total Environ (2017), http://dx.doi.org/10.1016/j.scitotenv.2017.03.025

3.4. MBC biodegradation analysis in the presence and absence of RL

The OD_{600} of *Rhodococcus* sp. D-1 was slightly enhanced in the presence of 150 ppm RL (RL150); however, there were no obvious effects on bacterial growth with 50 ppm RL (RL50) (Fig. 3b). Notably, the highest degradation rate was observed with RL50, whereas degradation was inhibited with RL150 (Fig. 3a). Thus, we hypothesized that high dose RL may function as co-substrate to compete with MBC and inhibit biodegradation (Zhao et al., 2011), though RL could not be used as a sole carbon and energy source in this study. After 2 days of cultivation, the degradation efficiencies with RL0, RL50, and RL150 were 56.74%, 97.33%, and 0.01%, respectively. A previous report showed that high concentrations of RL could result in self-association and decrease the availability of free molecules for capping semiconducting nanoparticles (Hazra et al., 2013). Mathurasa et al. (2012) also suggested that low concentrations of sodium dihexylsulfosuccinate could enhance interaction of tributyltin with indigenous soil bacteria and facilitate biodegradation, whereas high doses may pose synergistic toxic effects to bacteria with tributyltin. MBC was rapidly degraded in presence of RL150 and caught up with the other groups along with cultivation. The overall biodegradation efficiencies were similar for all treatments as 98.20%, 100.00%, and 99.26% for RL0, RL50, and RL150, respectively. RL utilization might facilitate MBC biodegradation in a surfactant-mediated-uptake way (Zhao et al., 2011), or D-1 adjusted to high RL concentrations by altering its cellular characteristics. In absence of RL, D-1 degraded MBC at a relatively stable rate without an obvious lag phase, and metabolized most of MBC within 3 days. However, an initial lag phase was observed in the presence of RL, which was prolonged with the highest RL concentration. This finding indicated an adverse effect on initial MBC biodegradation in the presence of high RL, probably by an apparent interference in the interaction between microbial cells and the hydrophobic substrate (Zhang and Miller, 1994; Zhao et al., 2011). We performed a preliminary experiment with 30 ppm RL (RL30), which inhibited MBC biodegradation as compared to the control group (RL0) even at the end of cultivation (data not shown).

Moreover, surfactants may show different effects on biodegradation of hydrophobic organic compounds. In diesel oil biodegradation by *Pseudomonas stutzeri*, RL significantly enhanced degradation efficiency, while saponins caused cell aggregation and inhibited biodegradation (Kaczorek et al., 2012). Triton X-100 had the highest pyrene solubilization capacity and improved hexadecane degradation by enhancing the solubility, emulsification, or facilitating interfacial attachment of cells; however, degradation was inhibited due to accumulation of toxic metabolites (Zhong et al., 2016b). Tween 80 facilitated biodegradation since it can serve as carbon source for higher biomass generation; however, JBR515 (a mixture of monorhamnolipid and dirhamnolipid) decreased the specific growth and pyrene utilization rates (Ghosh et al., 2014). In our study, Triton X-100 hampered MBC biodegradation (Fig. S2). Moreover, surfactants are more effective in enhancing hydrophobic hydrocarbons desorption from contaminated soil with relatively low clay and higher organic carbon content (Salunkhe et al., 2014). Investigation of the role of RL may offer preliminary suggestions for the bioremediation of MBC-polluted sites.

3.5. MBC emulsification and solubilization

Emulsification produces minute droplets that are uniformly dispersed in the aqueous phase and alters optical properties. It provides a greater surface area for attachment and direct interfacial uptake, as well as uptake after dissolution. In Fig. 4a, absorbance was positively correlated with MBC concentration, while no absorbance variation was observed in the absence of MBC, demonstrating that RL does emulsify MBC to enhance bioavailability. In contrast, Mohanty and Mukherji (2013) reported rather different phenomena. In that study, Triton X-100 caused emulsification and favorable changes in cell surface characteristics that enhanced biodegradation, while JBR-515 enhanced bioavailability and biodegradation by micellar solubilization instead of emulsification. The aqueous solubility of MBC in MSM in the absence of RL was measured as 5.78 ± 0.70 ppm, which is close to a previous report (6.11 ± 0.45 ppm, at pH 7.0) (Ni et al., 2002). It was reported that RL could facilitate PAHs solubilization by several folds, and monorhamnolipid showed a greater solubilizing capacity than dirhamnolipid (Congiu et al., 2015; Zhang et al., 1997). Notably, emulsification does not definitely lead to solubilization. For instance, though Triton X-100 has good emulsifying property, unnoticeable increase of dichlorobenzene solubilization has been observed, resulting in molar solubilization ratio of only 0.17 (Pastewski et al., 2006). We observed similar results that the increase in MBC solubility was rather inconspicuous in the presence of increasing dose of RL (Fig. 4b). RL seemed to have no considerable effects on MBC solubilization in our study.

3.6. Cell surface characteristics of strain D-1

3.6.1. Effect of RL on cell surface hydrophobicity

CSH is a measure of bacterial adhesion to hydrocarbons and an important factor in hydrophobic compound degradation (Kaczorek et al.,

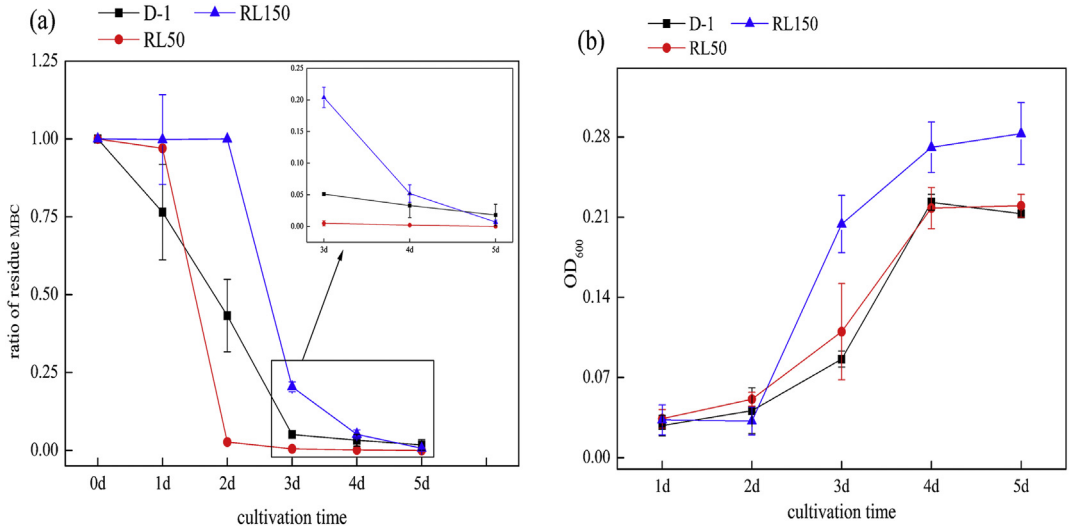

Fig. 3. Biodegradation analysis (a) and growth curve (b) of D-1 bacteria in cultures with various doses of RL. The initial MBC concentration was 200 ppm, which served as the sole carbon and energy source.

Please cite this article as: Bai, N., et al., Rhamnolipid-aided biodegradation of carbendazim by *Rhodococcus* sp. D-1: Characteristics, products, and phytotoxicity, Sci Total Environ (2017), http://dx.doi.org/10.1016/j.scitotenv.2017.03.025

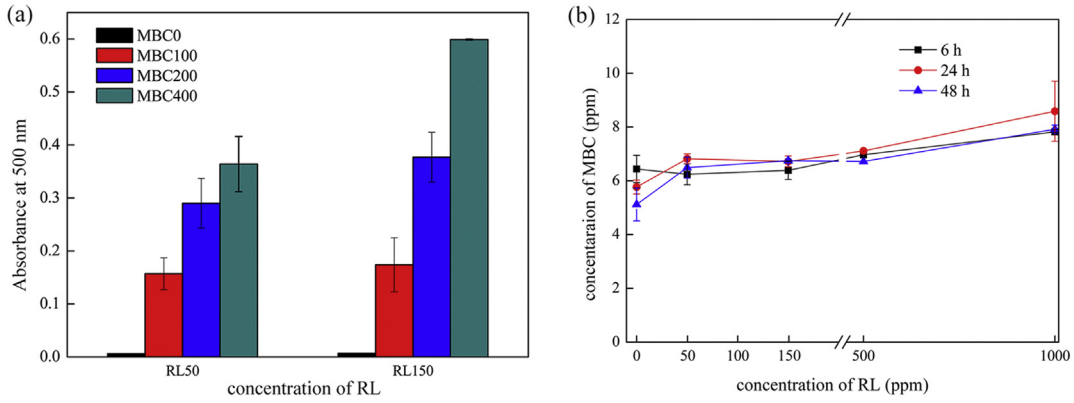

Fig. 4. (a) Emulsification analysis with increasing concentrations of MBC. (b) MBC solubility in presence of various doses of RL over time. Error bars represent standard error (SE) (1.5-column).

2012). In general, CSH stimulated the direct attachment of bacterial cells to various hydrophobic surfaces. The bacterial adhesion to hydrocarbon (BATH) assay is a measure of adherence affinity rather than hydrophobicity, and was not suitable for the direct analysis of CSH in MBC biodegradation (Ghosh and Mukherji, 2016). Water contact angle analysis on bacterial mats was used to overcome the limitations of the BATH assay. Notably, the analysis of RL-dependent effects on the CSH of *Rhodococcus* sp. D-1 at day 2 revealed marked changes in CSHs, as measured at 56.39°, 102.03°, and 84.74° after culturing with 0, 50, and 150 ppm RL, respectively (Fig. 5a) suggesting that the addition of RL had a remarkable influence on CSH (Zhong et al., 2008). This result was in contrast to a previous report, in which JBR515 decreased CSH to the hydrophilic range (≤30°) with the CSH of *B. multivorans* NG1 being 50°–60° in the absence of surfactant (Mohanty and Mukherji, 2013). It is also reported that RL can remove lipopolysaccharide from the outer bacterial membrane and subsequently expose hydrophobic phospholipid fatty acid tails, which then adsorb hydrophobic substances onto the cell surface (Zhao et al., 2011). Though addition of RL150 increased the CSH of D-1, the subsequent biodegradation of MBC was inhibited. In addition, the cell surface was moderately to highly hydrophobic in both RL cultures, as water contact angles >70° denote a highly hydrophobic cell surface (Mozes and Rouxhet, 1987). Hydrophobic surfaces increase the interaction between cells and hydrocarbon substrates, resulting in increased diffusion rates, substrate utilization, and cell growth in two-phase systems. In the stationary growth phase, the CSH in presence of RL50 and RL150 exhibited a sharp decrease to moderately hydrophobic. Moreover, the CSH remained stable of 60° ± 5° throughout the biodegradation period in absence of RL, similar to a previous report (Mohanty and Mukherji, 2012). Therefore, RL appeared to increase CSH to facilitate the adherence of particles and direct interfacial uptake.

Generally, surfactant may exhibit different mode of action depending on the composition of the pollutant and the culture used (Kaczorek et al., 2012). When D-1 was cultured with glucose as the sole carbon source, the CSH showed a relatively hydrophilic trend and decreased in the presence of RL (Fig. S3a), suggesting that the CSH varies depending on the carbon source used. The reduction of CSH may be attributed to the exposure of hydrophilic parts of RL to aqueous phase or the removal of extracellular hydrophobic substances from cell surface (Zhao et al., 2011). Similarly, Zhang and Miller (1994) noted that RL increases the CSH only when cells are incubated in the presence of the slightly soluble carbon sources.

3.6.2. Changes in zeta potential during biodegradation

Zeta potential refers to electrokinetic potential at the interface of two planes and reflects the net charge on the surface of the microorganism. Thus, a higher negative zeta potential is indicative of a higher negative surface charge. In the absence of RL, the zeta potentials of *Rhodococcus* sp. D-1 were −28.53, −20.9 and −33.1 mV at days 1, 3 and 5, respectively, which was further lowered with increasing concentrations of RL (Fig. 5b). The decrease in electronegativity of the cell surface favored MBC adherence and thus facilitated biodegradation (Mohanty and Mukherji, 2013). The zeta potentials in RL0 and RL50 cultures were higher at day 5 when compared to day 3. The zeta potential of D-1 seemed to decline in the presence of RL and during cultivation when the sole carbon source was changed to glucose (Fig. S3b). Moreover, all samples possessed relatively low zeta potentials ranging from −12.85 to −24.8 mV. Generally, different surfactants may exhibit

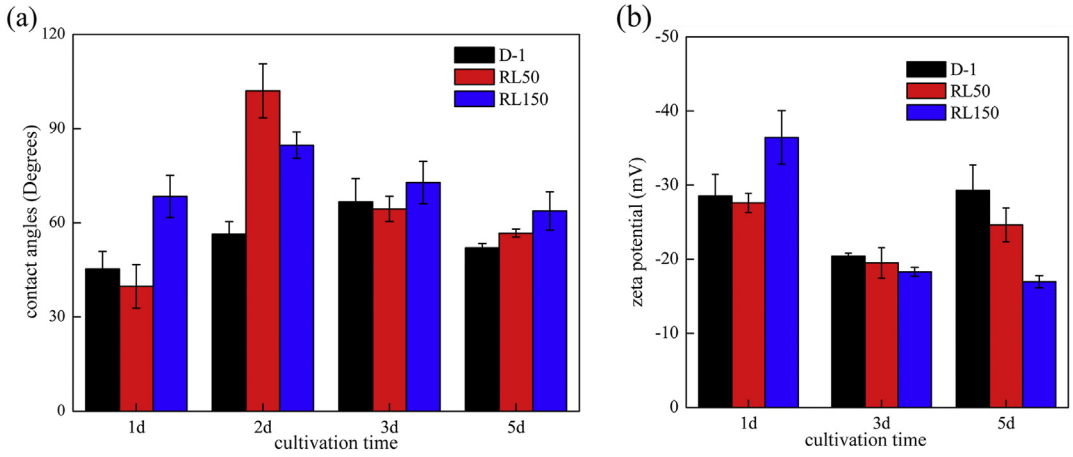

Fig. 5. (a) Changes of CSH and (b) zeta potential of *Rhodococcus* sp. D-1 with varying doses of RL.

Please cite this article as: Bai, N., et al., Rhamnolipid-aided biodegradation of carbendazim by *Rhodococcus* sp. D-1: Characteristics, products, and phytotoxicity, Sci Total Environ (2017), http://dx.doi.org/10.1016/j.scitotenv.2017.03.025

different effects on the zeta potential (Mohanty and Mukherji, 2012). Mohanty and Mukherji (2013) also pointed that pollutant composition affects cell surface characteristics, including CSH and zeta potential.

3.6.3. SEM images

SEM images revealed distinct changes in cell size, cell surface characteristics, and adsorption (Fig. 6). Notably, cells cultured in nutrient LB medium were smooth and short rod-shaped (0.5–2 μm wide × 1.2–5 μm long), but tended to be slender and plicated when cultured in MSM media with or without RL (0.4–0.6 μm wide × 1.2–3.7 μm long), manifesting as a 30% and 73% reduction in width and length. The degree of morphologic change of the cell surface was generally consistent with CSH variation. Furthermore, more profound cell deformation occurred with increasing concentrations of RL, suggesting that cells may rupture with further cultivation. Moreover, MBC particles (shown as white dots in the SEM images) were supposedly adsorbed onto the cell surface to varying degrees depending on RL concentration.

3.6.4. FTIR analysis

The changes in functional groups were preliminarily investigated using FTIR (Fig. 7). The FTIR peaks at 2924 and 2852 cm^{-1} indicate the C—H stretching vibrations of the extended hydrocarbon chain (Hazra et al., 2013). Peaks around 3300 cm^{-1} represent intermolecular hydrogen bonded O—H, while those around 1400 cm^{-1} correspond to the in-plain bending vibration of saturated alcohols. Moreover, deformation vibrations near 1650 cm^{-1} and 1542 cm^{-1} denote C═O and N—H/C—N bonds in the amide group, respectively, which correspond to classical peptide linkages. Peaks in the range of 1250–1000 cm^{-1} likely represented stretching vibrations in C—O (saturated alcohols), C—O—C (ethers or esters), C—C (ketones), and C—N (amines) (Sahoo et al., 2010). In general, remarkable differences were observed in cells cultured with RL50 and RL150 when compared with RL0 samples, as the 3300 and 1398 cm^{-1} peaks appeared sharper, while the valley at 1240 cm^{-1} was weaker in the presence of RL than the control group. Jiang (2011) previously reported on the formation of hydrogen bonds between the cell surface and hydrophobic substance, consistent with the specific larger and wider peaks at 3400, 1651, and 1548 cm^{-1} observed in the presence of RL. These results indicated that biochemical alterations of the cell surface facilitate MBC direct uptake biodegradation. Moreover, the pollutant may be more accessible to

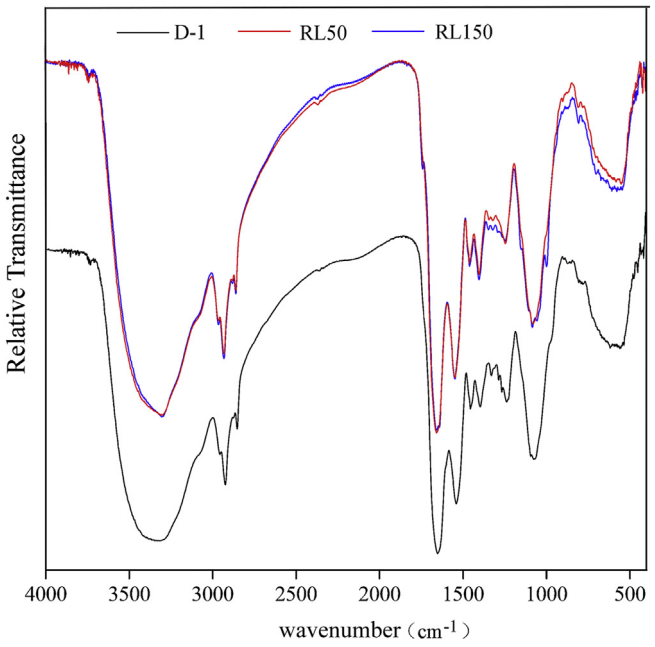

Fig. 7. FTIR analysis of strain D-1 in MBC degradation with different treatment.

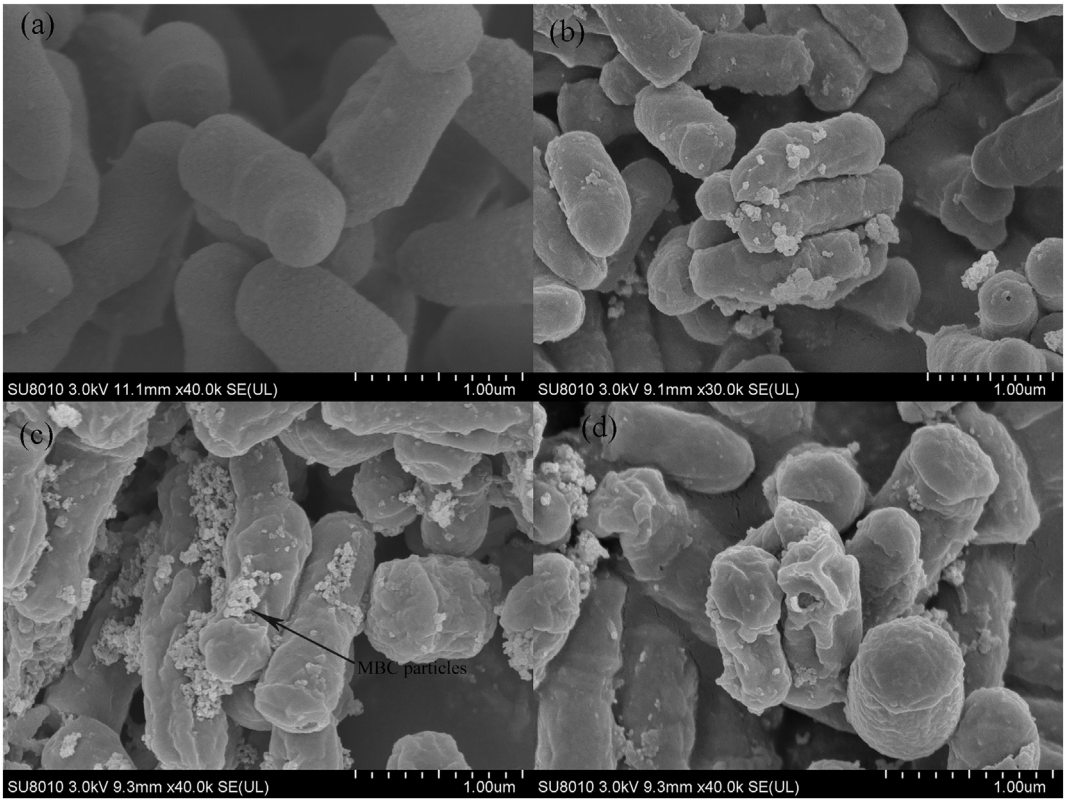

Fig. 6. SEM images of rod shaped *Rhodococcus* sp. D-1 in different cultivation conditions: (a) LB, (b) MSM with MBC, (c) MSM with MBC and RL50, (d) MSM with MBC and RL150. Scale bars, 1.00 μm.

Please cite this article as: Bai, N., et al., Rhamnolipid-aided biodegradation of carbendazim by *Rhodococcus* sp. D-1: Characteristics, products, and phytotoxicity, Sci Total Environ (2017), http://dx.doi.org/10.1016/j.scitotenv.2017.03.025

Table 2
Analysis of phytotoxicity tests.

	CK_{MSM}	0 d			2 d			3 d		
		RL0	RL50	RL150	RL0	RL50	RL150	RL0	RL50	RL150
Germination percentage	93 ± 7	97 ± 5	90 ± 1	69 ± 1**	84 ± 1	97 ± 1	73 ± 19*	83 ± 4	81 ± 0	79 ± 12
Shoot length (cm)	1.23 ± 0.13	0.4 ± 0.14***	0.175 ± 0.11***	0.25 ± 0.07***	0.3 ± 0.18***	0.55 ± 0.07**	0.15 ± 0.07***	0.8 ± 0.28*	1.125 ± 0.18	0.85 ± 0.49
Root length (cm)	0.5 ± 0.13	0.125 ± 0.11**	0.05 ± 0.07***	0.1 ± 0.14**	0.2 ± 0.28*	0.45 ± 0.07	0.125 ± 0.04**	0.45 ± 0.07	0.7 ± 0.01	0.275 ± 0.18*

The data are means of duplicate experiments ± SE. Significantly different from control groups at $p \le 0.05$ *, $p \le 0.01$ **, $p \le 0.001$ *** by one-way ANOVA analysis.

attached bacteria than suspended ones, which could enhance the mineralization rates under bioavailability restrictions (Tejeda-Agredano et al., 2014). So the increased mineralization rate in the presence of RL could be attributed to an additional passive contamination flow towards bacterial cells. Though RL did not enhance the partitioning of MBC, it did promote cell adhesion to MBC.

3.7. Phytotoxicity studies

MBC is widely used as pesticide in agriculture, and thus the accumulation of MBC is likely to affect soil characteristics and the plant seeds. Moreover, sometimes the biodegradation intermediates might be more toxic than the parent pollutant. Therefore, we determined changes in phytotoxicity during MBC biodegradation (Table 2). The germination percentage was not significantly affected by MBC or its degradation products with RL0 and RL50 ($p > 0.05$). However, the germination rate was significantly decreased in the presence of 150 ppm RL, which may be due to the emulsification effect of RL. Moreover, toxicity slightly decreased along with MBC biodegradation (germination rate was 79 ± 12 with biodegradation solution at Day 3). The growth of shoots and roots of Chinese cabbage was significantly inhibited by MBC; the inhibition was somewhat alleviated along with MBC biodegradation ($p < 0.05$). Furthermore, the shoot appeared to be more sensitive to MBC than the roots, which tended to be black, especially in the RL150 group (Day 0 and 2), indicating that MBC might significantly affect the root growth or other nutrient transformation (data not shown). RL facilitated rapid MBC biodegradation and detoxification, and such characteristics are desirable to be used for application purpose.

Generally, the dissipation rate of pollutants, including MBC, in natural environments is affected by biotic and abiotic factors and may vary from season to season and location to location (Salunkhe et al., 2014; Singh et al., 2016). Thus, microbial strains capable of degrading MBC under experimental conditions may not perform well *in situ*. As such, our next work will focus on analyzing the factors affecting MBC biodegradation in the environment.

4. Conclusion

The *Rhodococcus* D-1 strain capable of utilizing MBC as the sole carbon and energy source was isolated by continuous enrichment. Notably, *Rhodococcus* sp. D-1 effectively degraded 98.20% 200 ppm MBC in 3 days, respectively, into the primary metabolites 2-AB and 2-HB. There might be a novel enzyme capable of hydrolyzing MBC to 2-AB by genomic analysis. Moreover, addition of the biodegradable biosurfactant RL (1 and 3 CMC) enhanced the potential of *Rhodococcus* sp. D-1 to degrade and detoxify MBC in a concentration-dependent manner, where low RL concentration (50 ppm) reached a maximum biodegradation rate and efficiency and 97.33% of 200 ppm MBC in 2 days. Conversely, the high RL concentration (150 ppm) initially blocked MBC utilization, shown as a prolonged lag phase in the MBC degradation curve. Further, analysis of the RL mechanism of action demonstrated that emulsification and favorable changes in cell surface hydrophobicity and zeta potential facilitated MBC biodegradation and detoxification by *Rhodococcus* sp. D-1.

Supplementary data to this article can be found online at http://dx.doi.org/10.1016/j.scitotenv.2017.03.025.

Conflict of interest

There is no conflict of interest to report.

Acknowledgements

This study was supported by the National Natural Science Foundation of China (41271335; 31470191), the Major State Basic Research Development Program of China (973 program) (2015CB150502).

References

Besemer, J., Lomsadze, A., Borodovsky, M., 2001. GeneMarkS: a self-training method for prediction of gene starts in microbial genomes. Implications for finding sequence motifs in regulatory regions. Nucleic Acids Res. 29, 2607–2618.
Chang, Y.-T., Chou, H.-L., Chao, H.-P., Chang, Y.-J., 2015. The influence of sorption on polyaromatic hydrocarbon biodegradation in the presence of modified nonionic surfactant organoclays. Int. Biodeterior. Biodegrad. 102, 237–244.
Congiu, E., Parsons, J.R., Ortega-Calvo, J.-J., 2015. Dual partitioning and attachment effects of rhamnolipid on pyrene biodegradation under bioavailability restrictions. Environ. Pollut. 205, 378–384.
Dai, Shugui, Dong, Liang, 1999. Study progress on surfactant-enhanced remediation of contaminated environment. Shanghai Environmental Science 18, 420–424 (in Chinese).
Fang, H., Wang, Y., Gao, C., Yan, H., Dong, B., Yu, Y., 2010. Isolation and characterization of *Pseudomonas* sp. CBW capable of degrading carbendazim. Biodegradation 21, 939–946.
Fernando Bautista, L., Sanz, R., Carmen Molina, M., González, N., Sánchez, D., 2009. Effect of different non-ionic surfactants on the biodegradation of PAHs by diverse aerobic bacteria. Int. Biodeterior. Biodegrad. 63, 913–922.
Gardner, P.P., Daub, J., Tate, J.G., Nawrocki, E.P., Kolbe, D.L., Lindgreen, S., et al., 2009. Rfam: updates to the RNA families database. Nucleic Acids Res. 37, D136–D140.
Ghosh, I., Mukherji, S., 2016. Diverse effect of surfactants on pyrene biodegradation by a *Pseudomonas* strain utilizing pyrene by cell surface hydrophobicity induction. Int. Biodeterior. Biodegrad. 108, 67–75.
Ghosh, I., Jasmine, J., Mukherji, S., 2014. Biodegradation of pyrene by a *Pseudomonas aeruginosa* strain RS1 isolated from refinery sludge. Bioresour. Technol. 166, 548–558.
Guha, S., Jaffé, P.R., 1996. Bioavailability of hydrophobic compounds partitioned into the micellar phase of nonionic surfactants. Environ. Sci. Technol. 30, 1382–1391.
Hazra, C., Kundu, D., Chaudhari, A., Jana, T., 2013. Biogenic synthesis, characterization, toxicity and photocatalysis of zinc sulfide nanoparticles using rhamnolipids from *Pseudomonas aeruginosa* BS01 as capping and stabilizing agent. J. Chem. Technol. Biotechnol. 88, 1039–1048.
Holtman, M., Kobayashi, D., 1997. Identification of *Rhodococcus erythropolis* isolates capable of degrading the fungicide carbendazim. Appl. Microbiol. Biotechnol. 47, 578–582.
Jiang, P., 2011. Effect of Biosurfactant on Pyrene Degradation by *Pseudomonas* sp. GP3A. South China University of Technology (in Chinese).
Jing-Liang, X., Xiang-Yang, G., Biao, S., Zhi-Chun, W., Kun, W., Shun-Peng, L., 2006. Isolation and characterization of a carbendazim-degrading *Rhodococcus* sp. djl-6. Curr. Microbiol. 53, 72–76.
Kaczorek, E., Jesionowski, T., Giec, A., Olszanowski, A., 2012. Cell surface properties of *Pseudomonas stutzeri* in the process of diesel oil biodegradation. Biotechnol. Lett. 34, 857–862.
Lagesen, K., Hallin, P., Rødland, E.A., Stærfeldt, H.-H., Rognes, T., Ussery, D.W., 2007. RNAmmer: consistent and rapid annotation of ribosomal RNA genes. Nucleic Acids Res. 35, 3100–3108.
Lee, S., Kweon, J.H., Kim, H.S., 2013. Selective biodegradation of sorbitan ethoxylated surfactants by soil microorganisms. Int. Biodeterior. Biodegrad. 85, 652–660.
Lei, J., Ren, L., Hu, S., Ron, C.H., 2016. Isolation and characterization of the carbendazim-degrading strain djl-5B. Nat. Environ. Pollut. Technol. 15 (1), 97–102.
Lewandowska, A., Walorczyk, S., 2010. Carbendazim residues in the soil and their bioavailability to plants in four successive harvests. Pol. J. Environ. Stud. 19, 757–761.

Lowe, T.M., Eddy, S.R., 1997. tRNAscan-SE: a program for improved detection of transfer RNA genes in genomic sequence. Nucleic Acids Res. 25, 955–964.
Martínková, L., Uhnáková, B., Pátek, M., Nešvera, J., Křen, V., 2009. Biodegradation potential of the genus *Rhodococcus*. Environ. Int. 35, 162–177.
Mathurasa, L., Tongcumpou, C., Sabatini, D.A., Luepromchai, E., 2012. Anionic surfactant enhanced bacterial degradation of tributyltin in soil. Int. Biodeterior. Biodegrad. 75, 7–14.
Mohanty, S., Mukherji, S., 2012. Alteration in cell surface properties of *Burkholderia* spp. during surfactant-aided biodegradation of petroleum hydrocarbons. Appl. Microbiol. Biotechnol. 94, 193–204.
Mohanty, S., Mukherji, S., 2013. Surfactant aided biodegradation of NAPLs by *Burkholderia multivorans*: comparison between Triton X-100 and rhamnolipid JBR-515. Colloids Surf. B: Biointerfaces 102, 644–652.
Morinaga, H., Yanase, T., Nomura, M., Okabe, T., Goto, K., Harada, N., et al., 2004. A benzimidazole fungicide, benomyl, and its metabolite, carbendazim, induce aromatase activity in a human ovarian granulose-like tumor cell line (KGN). Endocrinology 145, 1860–1869.
Mozes, N., Rouxhet, P.G., 1987. Methods for measuring hydrophobicity of microorganisms. J. Microbiol. Methods 6, 99–112.
Ni, N., Sanghvi, T., Yalkowsky, S.H., 2002. Solubilization and preformulation of carbendazim. Int. J. Pharm. 244, 99–104.
Pandey, G., Dorrian, S.J., Russell, R.J., Brearley, C., Kotsonis, S., Oakeshott, J.G., 2010. Cloning and biochemical characterization of a novel carbendazim (methyl-1*H*-benzimidazol-2-ylcarbamate)-hydrolyzing esterase from the newly isolated *Nocardioides* sp. strain SG-4G and its potential for use in enzymatic bioremediation. Appl. Environ. Microbiol. 76, 2940–2945.
Pastewski, S., Hallmann, E., Medrzycka, K., 2006. Physicochemical aspects of the application of surfactants and biosurfactants in soil remediation. Environ. Eng. Sci. 23, 579–588.
Pornsunthorntawee, O., Chavadej, S., Rujiravanit, R., 2009. Solution properties and vesicle formation of rhamnolipid biosurfactants produced by *Pseudomonas aeruginosa* SP4. Colloids Surf. B: Biointerfaces 72, 6–15.
Sahoo, S., Datta, S., Biswas, D., Banik, Choudhury R., 2010. Biosurfactant production from n-paraffins by an air isolate *Pseudomonas aeruginosa* OCD_1. J. Oleo Sci. 59, 601–605.
Salunkhe, V.P., Sawant, I.S., Banerjee, K., Wadkar, P.N., Sawant, S.D., Hingmire, S.A., 2014. Kinetics of degradation of carbendazim by *B. subtilis* strains: possibility of in situ detoxification. Environ. Monit. Assess. 186, 8599–8610.
Sánchez-Camazano, M., Arienzo, M., Sánchez-Martín, M.J., Crisanto, T., 1995. Effect of different surfactants on the mobility of selected non-ionic pesticides in soil. Chemosphere 31, 3793–3801.
Singh, S., Singh, N., Kumar, V., Datta, S., Wani, A.B., Singh, D., et al., 2016. Toxicity, monitoring and biodegradation of the fungicide carbendazim. Environ. Chem. Lett. 14, 317–329.
Sun, P., Hui, C., Azim Khan, R., Du, J., Zhang, Q., Zhao, Y.-H., 2015. Efficient removal of crystal violet using Fe_3O_4-coated biochar: the role of the Fe_3O_4 nanoparticles and modeling study their adsorption behavior. Sci. Report. 5, 12638.
Tamura, K., Dudley, J., Nei, M., Kumar, S., 2007. MEGA4: molecular evolutionary genetics analysis (MEGA) software version 4.0. Mol. Biol. Evol. 24, 1596–1599.
Tejeda-Agredano, M.-C., Mayer, P., Ortega-Calvo, J.-J., 2014. The effect of humic acids on biodegradation of polycyclic aromatic hydrocarbons depends on the exposure regime. Environ. Pollut. 184, 435–442.
Wang, X., Song, M., Gao, C., Dong, B., Zhang, Q., Fang, H., et al., 2009. Carbendazim induces a temporary change in soil bacterial community structure. J. Environ. Sci. 21, 1679–1683.
Yenjerla, M., Cox, C., Wilson, L., Jordan, M.A., 2009. Carbendazim inhibits cancer cell proliferation by suppressing microtubule dynamics. J. Pharmacol. Exp. Ther. 328, 390–398.
Zhang, Y., Miller, R.M., 1994. Effect of a *Pseudomonas* rhamnolipid biosurfactant on cell hydrophobicity and biodegradation of octadecane. Appl. Environ. Microbiol. 60, 2101–2106.
Zhang, Y., Maier, W.J., Miller, R.M., 1997. Effect of rhamnolipids on the dissolution, bioavailability, and biodegradation of phenanthrene. Environ. Sci. Technol. 31, 2211–2217.
Zhang, Z.-X., Zhu, Y.-X., Li, C.-M., Zhang, Y., 2012. Investigation into the causes for the changed biodegradation process of dissolved pyrene after addition of hydroxypropyl-β-cyclodextrin (HPCD). J. Hazard. Mater. 243, 139–145.
Zhang, X., Huang, Y., Harvey, P.R., Li, H., Ren, Y., Li, J., et al., 2013. Isolation and characterization of carbendazim-degrading *Rhodococcus erythropolis* djl-11. PLoS One 8, e74810.
Zhao, Z., Selvam, A., Wong, J.W.-C., 2011. Effects of rhamnolipids on cell surface hydrophobicity of PAH degrading bacteria and the biodegradation of phenanthrene. Bioresour. Technol. 102, 3999–4007.
Zhong H. Adsorption of Rhamnolipid Biosurfactant on Microorganisms and the Effect of the Adsorption on Cell Surface Hydrophobicity. Hunan University 2008 (in Chinese).
Zhong, H., Zeng, G.M., Liu, J.X., Xu, X.M., Yuan, X.Z., Fu, H.Y., et al., 2008. Adsorption of monorhamnolipid and dirhamnolipid on two *Pseudomonas aeruginosa* strains and the effect on cell surface hydrophobicity. Appl. Microbiol. Biotechnol. 79, 671–677.
Zhong, H., Liu, G., Jiang, Y., Brusseau, M.L., Liu, Z., Liu, Y., et al., 2016a. Effect of low-concentration rhamnolipid on transport of *Pseudomonas aeruginosa* ATCC 9027 in an ideal porous medium with hydrophilic or hydrophobic surfaces. Colloids Surf. B: Biointerfaces 139, 244–248.
Zhong, H., Wang, Z., Liu, Z., Liu, Y., Yu, M., Zeng, G., 2016b. Degradation of hexadecane by *Pseudomonas aeruginosa* with the mediation of surfactants: relation between hexadecane solubilization and bioavailability. Int. Biodeterior. Biodegrad. 115, 141–145.
Zhou, W., Zhu, L., 2007. Efficiency of surfactant-enhanced desorption for contaminated soils depending on the component characteristics of soil-surfactant-PAHs system. Environ. Pollut. 147, 66–73.

Please cite this article as: Bai, N., et al., Rhamnolipid-aided biodegradation of carbendazim by *Rhodococcus* sp. D-1: Characteristics, products, and phytotoxicity, Sci Total Environ (2017), http://dx.doi.org/10.1016/j.scitotenv.2017.03.025